



A Study of Wear and Corrosion Resistance of Arc-Sprayed Ni-Ti Composite Coatings

C.H. Chang, M.C. Jeng, C.Y. Su, and T.S. Huang

(Submitted November 17, 2010; in revised form June 21, 2011)

In this study, the corrosion and wear performance of Ni-Ti composite coatings with distinct parameters were investigated. The coatings were prepared by arc spraying with Ti and Ni wires fed synchronously. Structural, surface morphological, and compositional analyses of the Ni-Ti composite coatings were performed using microhardness, SEM/EDS, XRD, and DTA analysis. Electrochemical AC impedance and potentiodynamic polarization tests were carried out to examine the anticorrosion performance of the coating. Ball-on-disc dry wear tests based on the ASTM G99 standard were performed at room temperature to evaluate the antiwear properties. The DTA and XRD analysis results indicated that some intermetallic compounds such as TiNi₃ and Ni-Ti alloy were present within the Ni-Ti coating. The wear resistance of the Ni-Ti composite coating is superior to that of the Ni-sprayed coating but slightly inferior to that of the Ti-sprayed coating. The corrosion resistance of the arc-sprayed Ni-Ti coating is superior to that of Ti but inferior to that of Ni. The corrosion and wear performance of the composite coating are greatly influenced by the coating microstructure and thickness.

Keywords arc spraying, corrosion, Ni-Ti, wear

1. Introduction

Thermal spraying is a well-developed coating technique in which metallic or nonmetallic materials are melted and softened by either chemical or electrical energy and the molten droplets are subsequently atomized and impacted on a prepared substrate to develop a laminar coating. Over the past decade, the use of thermal spraying techniques has increased in the electronic, chemical, and aerospace industries because of the high deposition rate, low cost, and wide variety of suitable materials. The four main types of processes used are flame spraying, plasma spraying, arc spraying, and high-velocity oxy/fuel (HVOF) spraying.

Arc spraying is a commonly used coating technique in which single or dual wires of either similar or dissimilar materials are melted, atomized, and subsequently deposited on a pretreated surface to build up a metallic coating. The thermal energy required to melt the wire is produced by an electric arc developed at its tip with a temperature of about 5000 °C. A high volume of compressed air is

required to atomize the molten metallic droplets and deliver them to the surface to be coated. In comparison with flame spraying, twin-wire arc spraying is an economical coating process with high productivity. A wide range of metals, alloys, and cored wires may be used to apply different types of coatings such as corrosion-protection, antiwear, and resurfacing coatings (Ref 1-5).

Intermetallic compounds are usually hard and brittle, and they can be prepared by techniques such as self-propagating high-temperature synthesis (SHS), mechanical alloying, sintering, or laser cladding. Many studies have demonstrated that the Ni-Ti alloy and intermetallic compounds exhibit excellent resistance to wear and erosion because of pseudo-elasticity (Ref 6-10). Thermal spraying by plasma spraying, arc spraying, or HVOF is also an easier way to develop metal-ceramic composite coatings, alloy coatings, and intermetallic compound coatings (Ref 11-15). The preparation of intermetallic compounds using two dissimilar wires is rather difficult because of the different melting points of the wires. In this study, an arc-sprayed Ni-Ti composite coating obtained by using a twin-wire arc-spraying system with the Ti and Ni wires fed synchronously was investigated. These composite coatings are discussed and their coating characteristics, antiwear properties, and corrosion resistance performance are compared to those of pure Ni- and Ti-sprayed coatings.

2. Experimental

2.1 Experimental Apparatus and Procedure

We used the Sulzer Metco SmartArc spray system consisting of a power supply, a programmable logic control (PLC) panel, and an arc spray torch. The substrate

C.H. Chang and M.C. Jeng, Department of Mechanical Engineering, National Central University, Taoyuan, Taiwan, ROC; C.H. Chang, Chemical Systems Research Division, Chung-Shan Institute of Science & Technology, Lungtan, Taiwan, ROC; C.Y. Su, Department of Mechanical Engineering, National Taipei University of Technology, Taipei, Taiwan, ROC; and T.S. Huang, New Materials Research & Development Department, China Steel Corporation, Kaohsiung, Taiwan, ROC. Contact e-mail: j327.j327@msa.hinet.net.



used in this study was AISI 1020 low-carbon steel with thickness of 3 mm, and all the specimens to be coated were pretreated by grit blasting to a white metal finish to satisfy the Swedish standard SIS 05 59 00 level Sa3. The pretreated specimens were subsequently sprayed with dual Ni wires, dual Ti wires, and a combination of Ni and Ti wire, the wire and nozzle orifice size were 1.6 mm in diameter.

The nomenclature used for the specimens is A-B. Here, A stands for the arc-spraying voltage and current and is classified into three levels: L for low power, 25 V/120 A; M for medium power, 28 V/200 A; and H for high power, 32 V/300 A. B stands for the spraying pressure: 35 for 35 psi (2.38 kg/cm²) and 70 for 70 psi (4.76 kg/cm²). Ti and Ni coatings are prepared by arc spraying with the arc current of 200 A, arc voltage of 28 V, and the atomizing pressure of 50 psi (3.52 kg/cm²). The thicknesses of Ti and Ni coatings are in the range of 100-180 μ m.

2.2 Analysis of Coating Characteristics

We carried out numerous analyses and measurements, including microhardness (Matsuzawa MXT70) using a diamond indenter, with the shape of square-based pyramid with an angle of 136° between opposite faces. The test duration is 5 s and load force is 100 gf, coating thickness (Karl Deutsch Leptoskop 2040), surface roughness (Kosaka Lab SE1200), and SEM observations (Philips SL40), to study the characteristics of the coatings.

2.3 Corrosion Test

2.3.1 AC Impedance Test. An AutoLab PGSTAT30 impedance spectrometer was used for the AC impedance measurements over a scanning frequency range of 10⁻²-10⁵ Hz in 3.5 wt.% NaCl solutions. The tests were carried out in a three-electrode cell using a platinum counter electrode and an Ag/AgCl reference electrode. The tested area was 1 cm², and the specimens were immersed in the 3.5 wt.% NaCl solutions for 10 min prior to the test.

2.3.2 Potentiodynamic Polarization. A potentiostat (EG&G PARC model 273) and a frequency-response analyzer (EG&G PARC model 1025) were controlled by electrochemical corrosion test software (EG&G model 352) to measure the potentiodynamic polarization curves. The measurements were performed in a three-electrode cell having a platinum counter electrode and a saturated calomel electrode (SCE) as a reference electrode. The tested area was 7 cm² and the specimens were immersed in a 3.5 wt.% NaCl solution for 10 min to balance the potential prior to the test. The NaCl solution was prepared with deionized water (18 M Ω -cm) from the Millipore Milli-Q SP water purification system.

2.4 Ball-on-Plane Wear Test

The ball-on-plane wear test based on ASTM D6425-99 was performed at room temperature using the Schwingung Reibung Verschleiss (SRV oscillation friction wear) tester by moving a stationary ball back and forth on the tested specimen. The contact material was an AISI E52100

chromium steel ball with diameter 10 mm and an average hardness of HRC 60 \pm 2. The test conditions were as follows: sliding stroke, 0.9 mm; sliding frequency, 50 Hz; and normal load, 50 N. The test durations were 5, 10, 15, and 20 min, resulting in sliding distances of 13.5, 27, 40.5, and 54 m. The weight loss of the specimen after the test was measured by an electronic analytical balance (Mettler AT261) with a minimum reading of 0.01 mg.

3. Results and Discussion

3.1 Coating Characterization

3.1.1 SEM/EDS Observation. Surface and cross-sectional SEM micrographs of the arc-sprayed Ti coating are shown in Fig. 1(a) and (b). A number of microcracks were observed on both the surface and the cross section of the coating. A cross-sectional SEM micrograph of the arc-sprayed Ni-Ti coating is shown in Fig. 1(c). It is clear that the coating is a mixture of white and gray platelets that were identified as Ni and Ti, respectively, by EDS analysis. Surface SEM micrographs of the arc-sprayed Ni-Ti coating with different spraying parameters are shown in Fig. 2. There is no significant difference on coating appearance among these samples with different parameters. It was found that the coatings deposited with high atomizing pressure exhibit a more uniform mixture than those deposited with low atomizing pressure.

3.1.2 XRD Analysis. XRD analyses of the arc-sprayed Ni-Ti coatings with different spraying parameters are presented in Fig. 3. These coatings are composed of Ni, TiN, and Ni-Ti intermetallic compounds such as Ti₃Ni₄. However, there is insufficient information to show any composition differences.

3.1.3 Microhardness Measurement. The microhardness of Ni-Ti composite coatings with different spraying parameters is shown in Fig. 4. It was observed from Fig. 1(c) that the Ni-Ti composite coating has gray and white platelets. The microhardness of the gray platelet was found to be higher than that of the white one. The average microhardness value in the gray phase of Ni-Ti composite coating is HV 619.6, which is two or three times higher than that of the pure Ti coating (HV 339.4), pure Ni coating (HV 228.6), and AISI 1020 steel substrate (HV 136.7).

3.1.4 DTA Analysis. An H-35 specimen was analyzed by DTA and the result is shown in Fig. 5. The specimen was heated to 1410 °C at a rate of 20 °C/min. Three exothermic peaks were found. According to the phase diagram of Ni-Ti, the first peak at 1119.67 °C could be an eutectic point of the Ni-Ti alloy with 66 wt.% Ni and 34 wt.% TiNi₃ intermetallic compound. The other two exothermic peaks at 1294.12 and 1382.55 °C seem to be congruent melting points of Ni-Ti and TiNi₃, respectively. Given this result, it is assumed that some intermetallic compounds such as TiNi₃ and Ni-Ti were formed during the spraying process when the Ni and Ti wires were melted and struck the substrate. Analyses of L-35 and M-35 specimens show curves similar to that for H-35, but

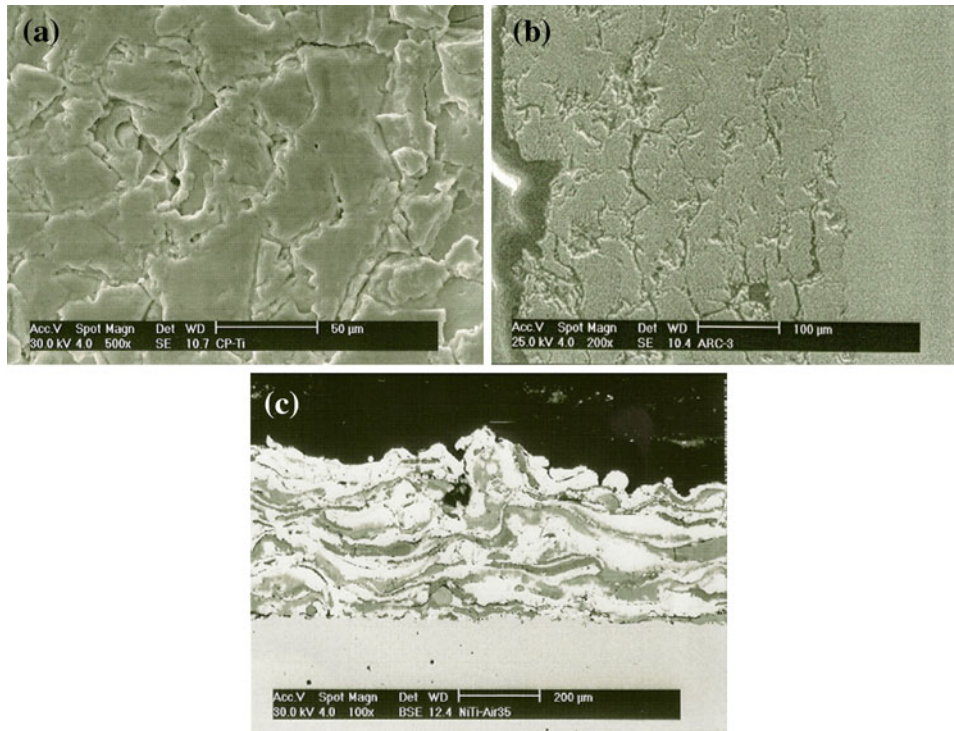


Fig. 1 SEM micrograph: (a) Ti coating, surface 500 \times ; (b) Ti coating, cross section 200 \times ; and (c) Ni-Ti composite coating, cross section 100 \times

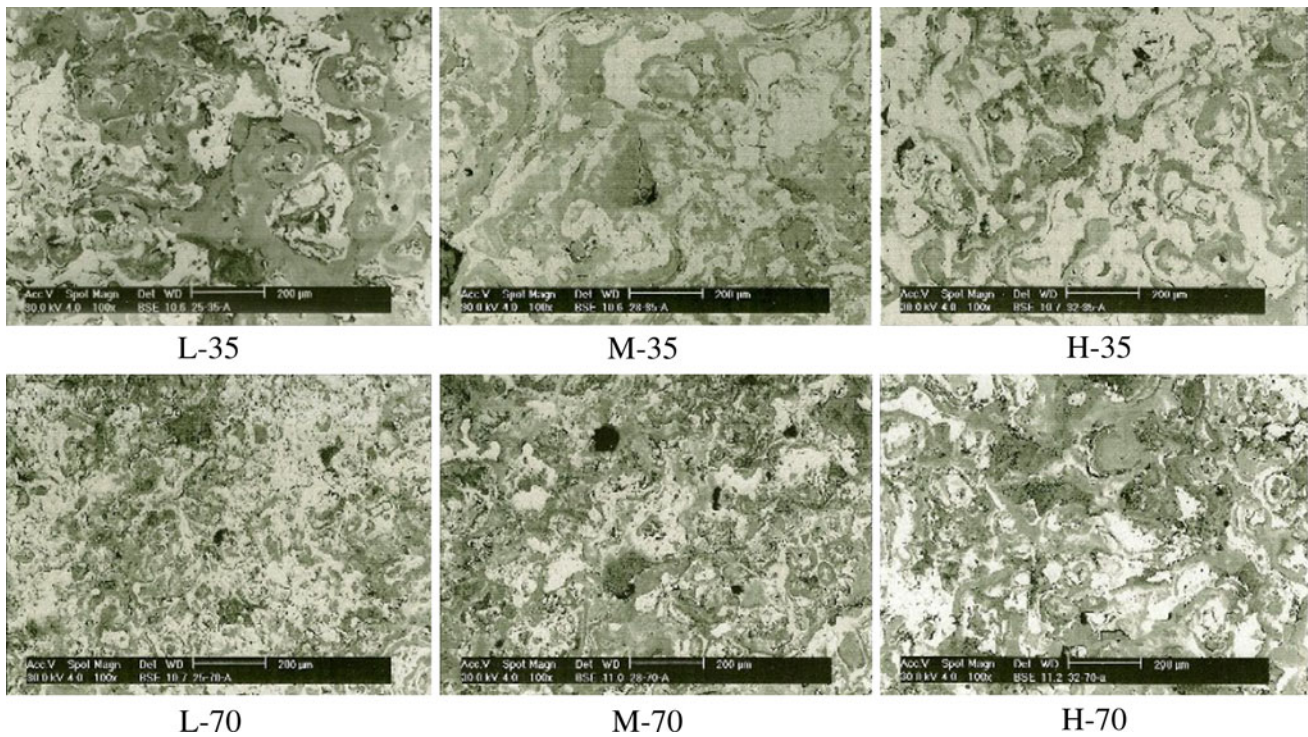


Fig. 2 Surface SEM micrograph of Ni-Ti composite coating (100 \times)

without the peak at 1119.67 °C. This suggests that the intermetallic compounds are formed only by high power. In this study, coatings made with medium- and low-power did not form intermetallic compounds.

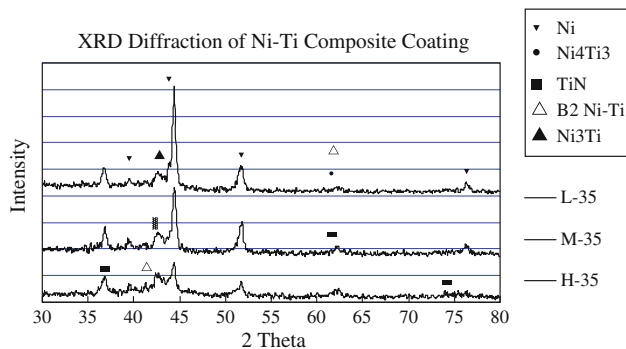


Fig. 3 XRD diffraction of Ni-Ti composite coating

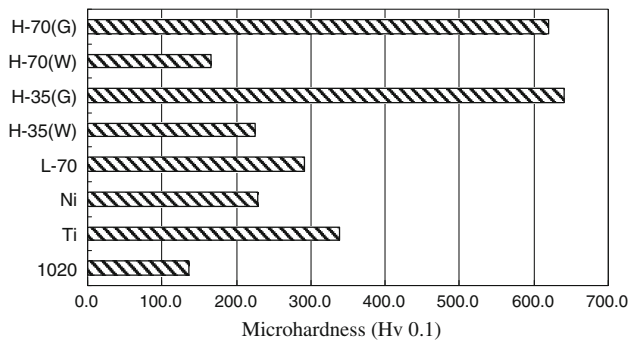


Fig. 4 Microhardness analysis results for Ni-Ti composite coating

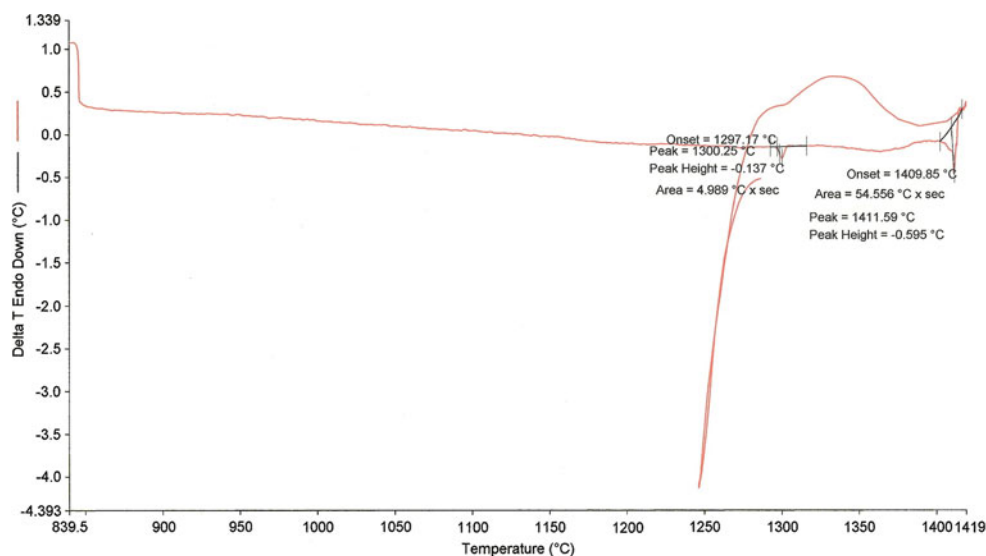


Fig. 5 DTA analysis results for Ni-Ti composite coating (H-35)

3.2 Corrosion Resistance

3.2.1 AC Impedance Test. Pure Ni coating and pure Ti coating, as well as AISI 1020 low-carbon steel substrate, were first tested for their AC impedance properties. It is seen from Fig. 6(a) that Ni coating has the highest impedance value and Ti coating, the lowest. In general, a higher impedance value indicates a higher resistance to corrosion. The results of AC impedance tests on Ni-Ti composite coatings with different spraying parameters are shown in Fig. 6(b) and (c). Although the impedance values are not identical at low frequencies, they lie between the values of the Ni and Ti coatings. It is seen from Fig. 6(b) that there is little difference in the impedance values of those sprayed at low pressure. However, a difference can be seen for those sprayed at high pressure (Fig. 6c). Two L-70 specimens, one 47 μm and the other 96 μm in thickness, illustrate the different impedance values. It is likely that the impedance value depends on the coating thickness: the thicker the coating, the larger is the impedance value.

Metal coatings can be classified into two groups, either noble or sacrificial. In this study Ni, Ti and Ni-Ti coatings are more positive (noble) than carbon steel, a potential difference exists between metal coatings and base material. Contrary to sacrificial coatings, the coating thickness and degree of porosity for noble coatings is relatively important. The AC experimental results reveal that the thicker the coating, the better protection will be provided to the substrate. All metal coatings contain lots of defects such as porosity, cracks, and oxide content. As SEM micrographs shown in Fig. 1(a) and (b), a number of microcracks were observed on both the surface and the cross section of Ti coating. It is assumed that these defects of Ti coating can result in a decrease in corrosion resistance.

3.2.2 Potentiodynamic Polarization Test. The potentiodynamic polarization curves of thermal-sprayed Ni, Ti,

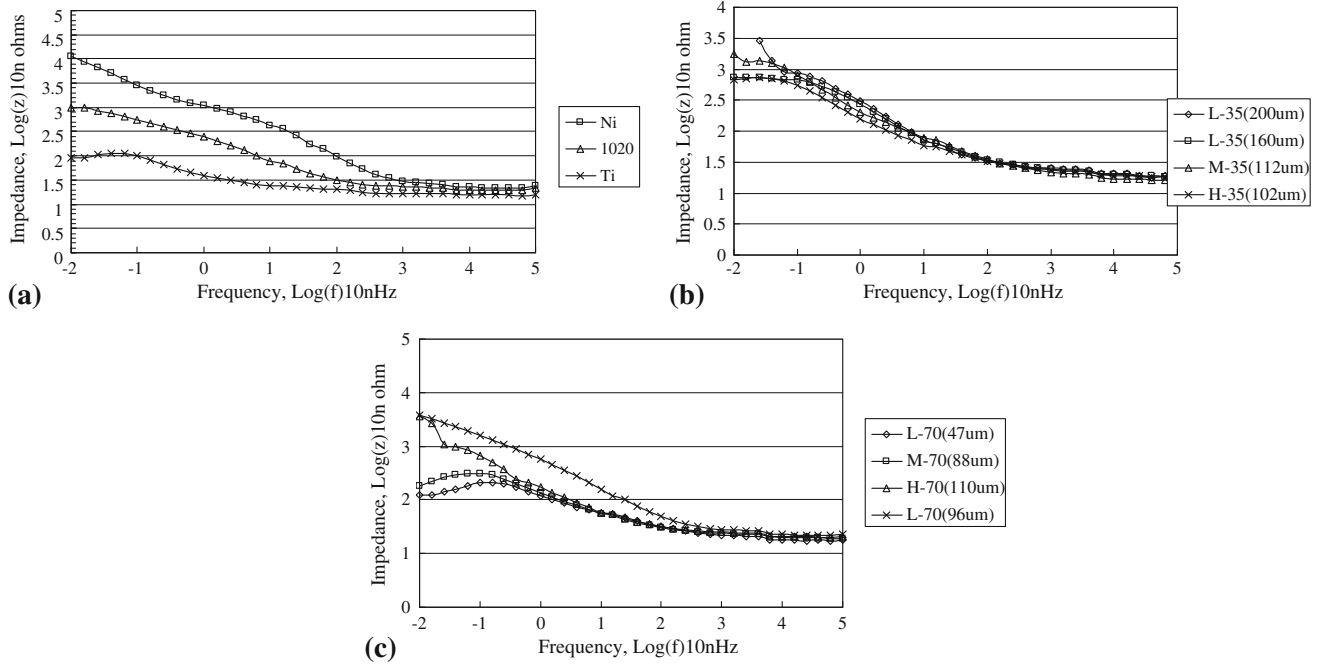


Fig. 6 AC impedance test results for Ni-Ti composite coating

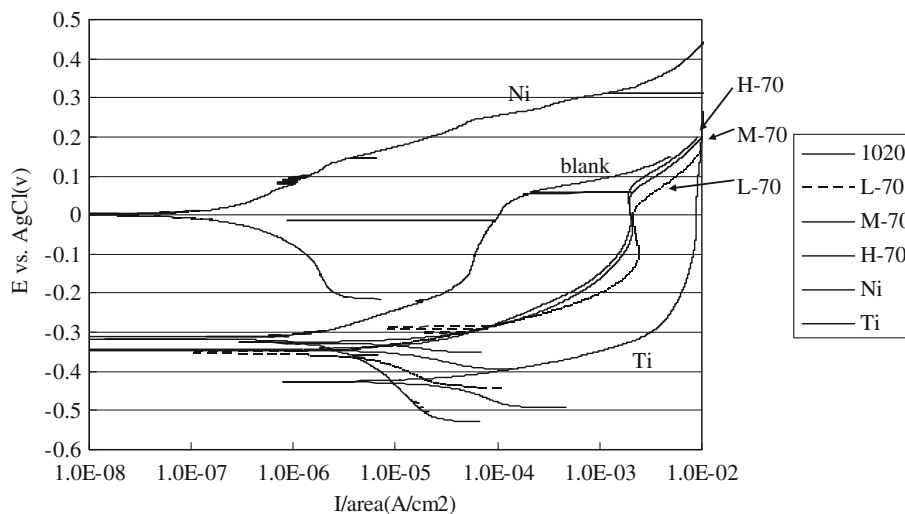


Fig. 7 Potentiodynamic polarization curves for thermal-sprayed Ni, Ti, and Ni-Ti coating

and Ni-Ti composite coatings are shown in Fig. 7. Ni coating has the highest corrosion potential and Ti coating, the lowest. In general, the higher the corrosion potential, higher is the corrosion resistance of the material. The corrosion resistance of the Ni-Ti composite coating is superior to that of the Ti coating and inferior to that of the Ni coating. This is consistent with the AC impedance test results presented in Section 3.2.1. The corrosion potential of AISI 1020 low-carbon steel substrate is slightly higher than those of the Ni-Ti composite coatings. The passivation current density of the steel substrate is also lower than those of the Ni-Ti composite coatings. Therefore,

Ni-Ti composite coatings sprayed on AISI 1020 low-carbon steel substrate act as an artificial coating to protect the substrate.

3.3 Ball-on-Plate Wear Test

The ball-on-plate test results are presented in Fig. 8-10, and SEM micrographs of the surface morphologies after the wear tests are shown in Fig. 11 and 12. The antiwear properties of the composite coating were evaluated by the wear rate, which is defined as the ratio of weight loss to the traveling distance. A comparison of the wear resistance of

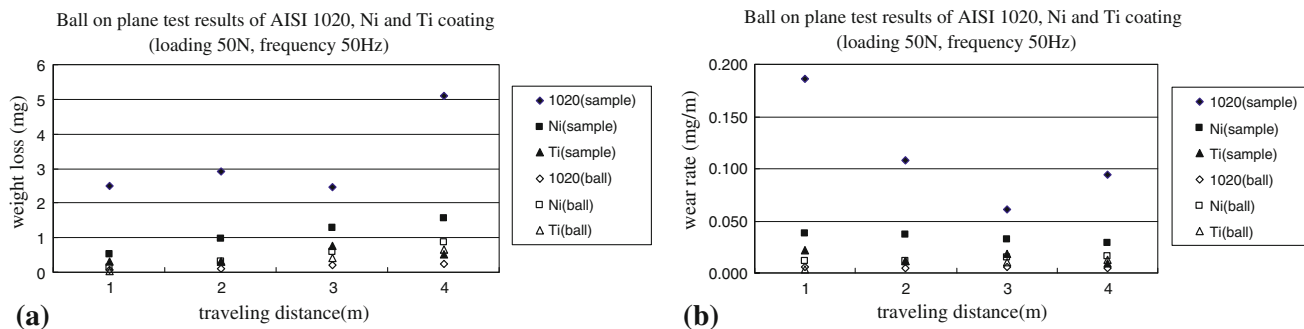


Fig. 8 ASTM D6425-99 wear test results for AISI 1020 and thermal-sprayed Ni and Ti coatings (a) weight loss and (b) wear rate

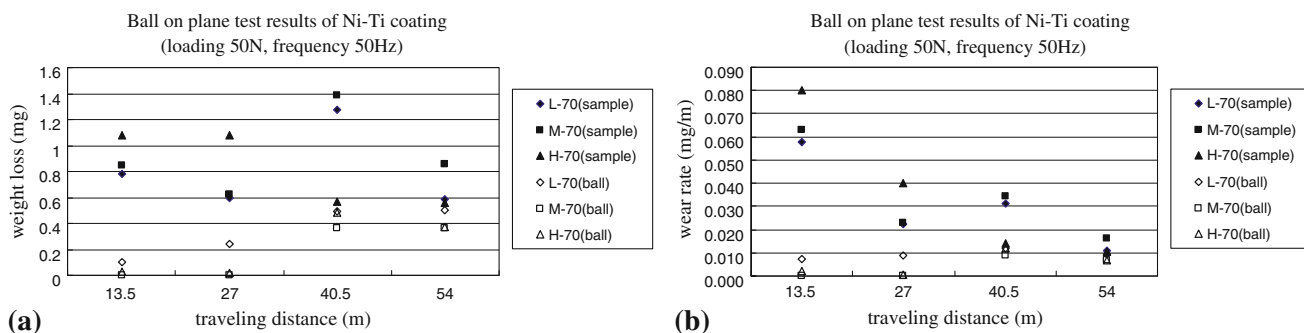


Fig. 9 ASTM D6425-99 wear test results for thermal-sprayed Ni-Ti composite coating (loading 50 N) (a) weight loss and (b) wear rate

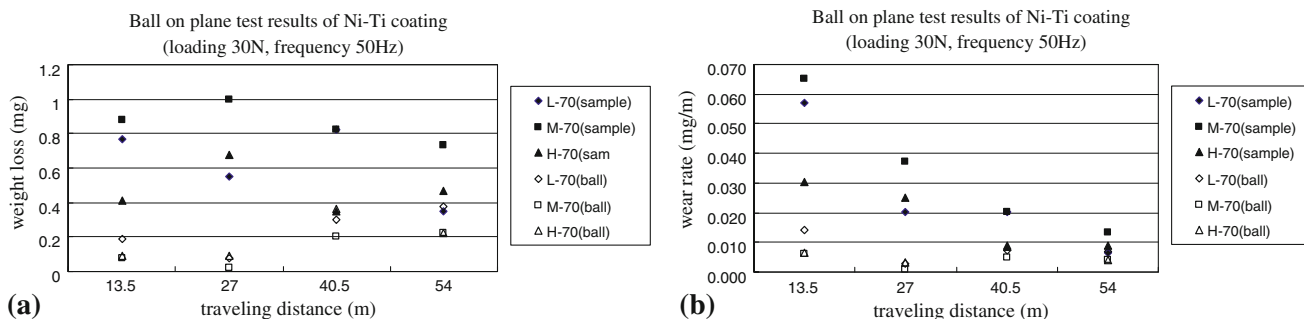


Fig. 10 ASTM D6425-99 wear test results for thermal-sprayed Ni-Ti composite coating (loading 30 N) (a) weight loss and (b) wear rate

AISI 1020 substrate, arc-sprayed Ni coating, and Ti coating is presented in Fig. 8. The friction coefficients between the tested specimens and the balls range from 0.09 to 0.12. The weight losses of both specimens and the ball increased with traveling distance, but the wear rates are decreased due to lower contact stress. The arc-sprayed Ti coating has an average wear rate of 0.014 mg/m, which is much lower than that of the Ni coating (0.032 mg/m) and AISI 1020 steel (0.096 mg/m).

The average weight losses of the Ni-Ti composite coatings with 50 N loading are shown in Fig. 9. The weight loss of the homogeneous steel ball increases steadily with traveling distance. However, the weight loss of the coating is more complicated. Because of the nonhomogeneous and

laminar characteristics of thermal-sprayed coatings, the wear behavior of Ni-Ti coatings is driven by its coating structure and by defects such as microcracks and porosity; these are markedly influenced by the spraying parameters such as atomizing pressure and arc current and voltage. The effects of porosity, flattening ratio, oxide content, and splat-to-splat bonding strength play an important role to coating antiwear performance. Low cohesion and high porosity generally cause a large piece of the coating wear away and result in a decrease on the wear performance. A coating sprayed at a higher atomizing pressure exhibits a more uniform and dense structure and possesses excellent antiwear properties. The average weight losses of the Ni-Ti composite coatings with 30 N loading are shown in

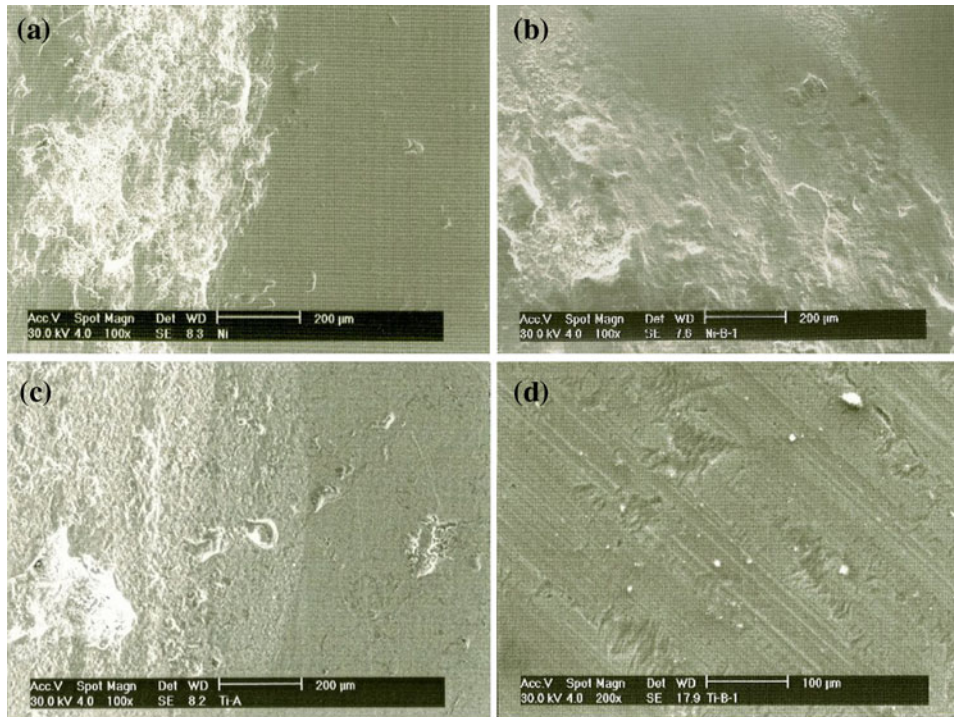


Fig. 11 SEM micrographs of thermal-sprayed Ni and Ti coatings after wear tests. (a) Ni (sample) 100×; (b) Ni (ball) 100×; (c) Ti (sample) 100×; and (d) Ti (ball) 200×

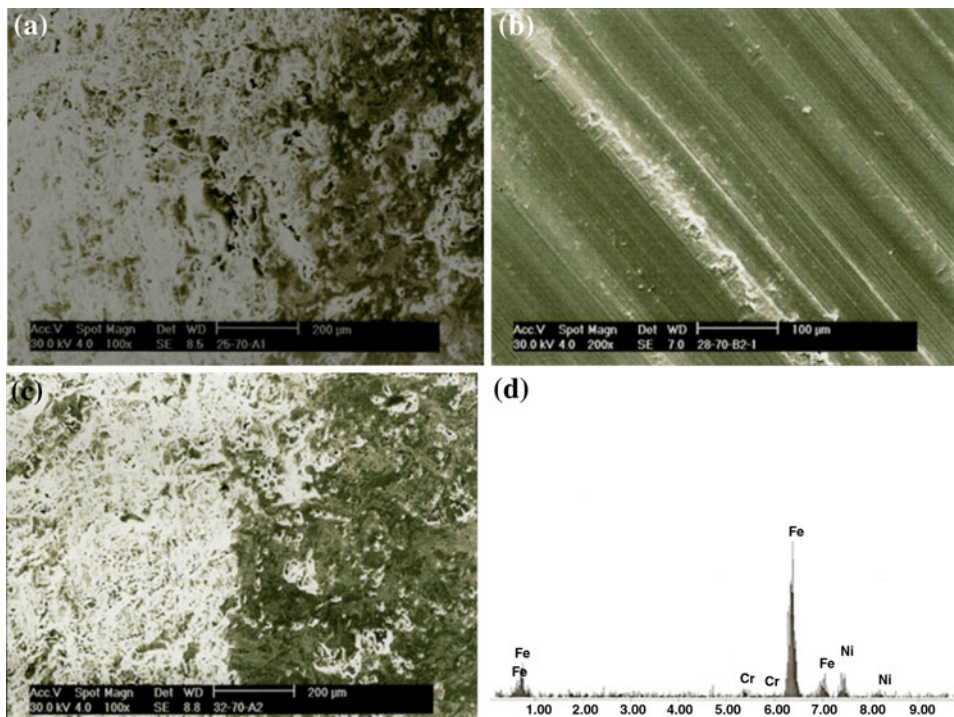


Fig. 12 SEM micrographs of thermal-sprayed Ni-Ti composite coating after wear tests (a) L-70 (sample) 100×; (b) M-70 (ball) 200×; (c) H-70 (sample) 200×; (d) EDS analysis of ball

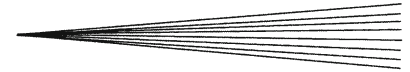


Fig. 10. Comparing Fig. 9 with Fig. 10, we find that the weight losses of the Ni-Ti composite coatings increased with loading force.

SEM micrographs of the Ni and Ti specimens after the wear tests are shown in Fig. 11(a) and (c). No significant microplothing or microcutting is observed for either specimen. The wear of the Ni and Ti specimens is assumed to be adhesive. Figure 11(b) and (d) show SEM micrographs of the steel ball after the wear tests on the Ni and Ti specimens. The EDS analysis shows that Ni was transferred from the Ni specimens to the steel ball, indicating adhesive wear. As shown in Fig. 11(d), the wear track of the steel ball tested on the Ti specimen shows a combination of adhesive and abrasive wear. Surface SEM micrographs of the Ni-Ti specimens after the wear tests are shown in Fig. 12(a) and (c). No significant microplothing or microcutting is observed for the Ni and Ti specimens. The wear of the specimens is assumed to be adhesive. Figure 12(b) shows an SEM micrograph of the steel ball after the wear tests on the Ni-Ti specimens. It also shows a combination of adhesive and abrasive wear. As shown in Fig. 12(d), the EDS analysis of the Ni-Ti specimen after the wear tests reveals that some Fe and Cr elements are transferred from the steel ball because of adhesive wear.

4. Conclusion

- (1) The surface analysis results show that a composite coating consisting of a Ni and Ti metal matrix and Ni-Ti intermetallic compounds such as Ti_3Ni_4 is developed by Ni-Ti arc-spraying process.
- (2) The experimental AC impedance results indicate that the corrosion resistance of arc-sprayed coatings is ranked in decreasing order as follows: Ni, Ni-Ti, and Ti. The anticorrosion performance of the arc-sprayed coating is found to depend on the coating structure and thickness. The potentiodynamic polarization test results are similar to the AC impedance results. The arc-sprayed Ni coating has a higher corrosion potential than the Ti and Ni-Ti coatings.
- (3) Evidence from the wear tests shows that the wear performance of the arc-sprayed Ti coating is superior to those of the Ni and Ni-Ti coatings.

References

1. E.R. Sampson, Thermal Spray Coatings for Corrosion Protection: An Overview, *Mater. Perform.*, 1997, **38**(12), p 27-30
2. B. Fitzsimons, Thermal Spray Metal Coatings for Corrosion Protection, *Corros. Manag.*, Dec. 1995/Jan. 1996, p 12-17
3. L.E. Weiss, F.B. Prinz, and E.L. Gursoz, Rapid Tool Manufacturing, U.S. Patent 5,189,781, 1993
4. L.E. Weiss, D.G. Thuel, L. Schultz, and F.B. Prinz, Arc Sprayed Steel-Faced Tooling, *J. Therm. Spray Technol.*, 1994, **3**(3), p 275-281
5. L.E. Weiss and F.B. Prinz, A Thermal Spray Approach to Rapid Prototyping—An Extended Abstract, *J. Therm. Spray Technol.*, 1994, **3**(3), p 297-298
6. A.P. Jardine, Y. Horan, and H. Herman, Cavitation Erosion Resistance of Thick Film Thermally Sprayed Ni-Ti High Temperature Ordered Intermetallic Alloys IV, *Proceedings of the 4th MRS Symposium*, Boston, MA, 27-30 Nov. 1990, p 815-820
7. L.M. Qian, Z.R. Zhou, and Q.P. Sun, The Role of Phase Transition in the Fretting Behavior of Ni-Ti Shape Memory Alloy, *Wear*, 2005, **259**, p 309-318
8. D.Y. Li, A New Type of Wear-Resistant Material: Pseudo-Elastic TiNi Alloy, *Wear*, 1998, **221**, p 116-123
9. D.Y. Li and R. Liu, The Mechanism Responsible for High Wear Resistance of Pseudo-Elastic TiNi Alloy—A Novel Tribo-Material, *Wear*, 1999, **225-229**, p 777-783
10. H.C. Lin, H.M. Liao, J.L. He, K.M. Lin, and K.C. Chen, Wear Characteristics of Ion-Nitrided $Ti_{50}Ni_{50}$ Shape Memory Alloys, *Surf. Coat. Technol.*, 1997, **92**, p 178-189
11. H. Hiraga, T. Inoue, H. Shimura, and A. Matsunawa, Cavitation Erosion Mechanism of NiTi Coatings Made by Laser Plasma Hybrid Spraying, *Wear*, 1999, **231**, p 272-278
12. T. Watanabe, T. Sato, and A. Nezu, Electrode Phenomena Investigation of Wire Arc Spraying for Preparation of Ti-Al Intermetallic Compounds, *Thin Solid Films*, 2002, **407**, p 98-103
13. N. Sakoda, M. Hida, Y. Takemoto, A. Sakakibara, and T. Tajiri, Influence of Atomization Gas on Coating Properties Under Ti Arc Spraying, *Mater. Sci. Eng. A*, 2003, **342**, p 264-269
14. B.S. Xu, Z.X. Zhu, S.N. Ma, W. Zhang, and W.M. Liu, Sliding Wear Behavior of Fe-Al and Fe-Al/WC Coatings Prepared by High Velocity Arc Spraying, *Wear*, 2004, **257**, p 1089-1095
15. J.A. Hearley, J.A. Little, and A.J. Sturgeon, The Erosion Behaviour of NiAl Intermetallic Coatings Produced by High Velocity Oxy-Fuel Thermal Spraying, *Wear*, 1999, **233-235**, p 328-333